10 Gbit/s 850 nm VCSEL Based Data Transmission over 100 m-long Multimode Photonic Crystal Fibers

Martin Stach*

Quasi error-free 10 Gbit/s data transmission is demonstrated over a novel type of 50 μm core diameter photonic crystal fiber with as much as 100 m length. Combined with 850 nm VCSEL sources, this fiber is an attractive alternative to graded-index multimode fibers for datacom applications. Comparative numerical simulations suggest that the high bit rate may be partly explained by inter-modal diffusion.

1. Introduction

Optical datacom as employed for the high-speed interconnection of electronic sub-systems has rapidly gained importance over the past years. Vertical-cavity surface-emitting lasers (VCSELs) emitting in the 850 nm wavelength regime and simple step-index fibers or graded-index fibers are preferred key components for low-cost link solutions [2]. Whereas, due to strong inter-modal dispersion, the use of the former fiber type is limited to link lengths of some meters at Gbit/s data rates, fabrication of the latter requires supreme control over the refractive index profile, especially in optimized 50 μm core diameter fibers enabling up to 300 m serial transmission of 10 Gbit/s signals. Since optical interconnect requirements move toward higher speed over shorter distances, the availability of an easily manufacturable, yet high-speed capable fiber medium would be very beneficial. This contribution reports on the properties of a new type of multimode photonic crystal fiber (PCF) fabricated by Crystal Fibre A/S. It features a simple waveguide geometry and allows 850 nm data transmission at 10 Gbit/s over a length of $L = 100$ m. For a recent review of photonic crystal fibers, the reader is referred to Ref. [3] and references therein.

2. Fiber Design

The design of the new multimode photonic crystal fiber is illustrated in the insets of Fig. 1 which show optical micrographs of the fiber cross-sections. The fibers are made from a single material (light regions), and they comprise a solid, pure silica core suspended in air (dark regions) by narrow silica bridges of width b. The waveguiding properties of the fiber may accurately be tailored by adjusting parameters such as the size and shape of the core, the dimensions and number of silica bridges, or the fiber material. The numerical

*Work performed in collaboration with Crystal Fibre A/S, Denmark; www.crystal-fibre.com; see [1] aperture (NA) of this type of PCF is essentially determined by the width of the silica bridges relative to the wavelength λ, as numerically demonstrated in Fig. 1. Here, we focus on two fibers with 33 µm and 50 µm core diameter and bridge widths of $b = 4.8$ µm and 7.0 µm, respectively, yielding NAs of around 0.07 and 0.05 at a wavelength of 850 nm. Despite the zero-index step between the core and the bridges, the fiber is capable of guiding light with good confinement to the multimode core. This is illustrated by the near-field intensity distribution for the 33 µm core PCF displayed in Fig. 5. The fibers can be cleaved with commercially available equipment and they have an attenuation of the order 50 dB/km at 850 nm for typical bending radii such as 16 cm.

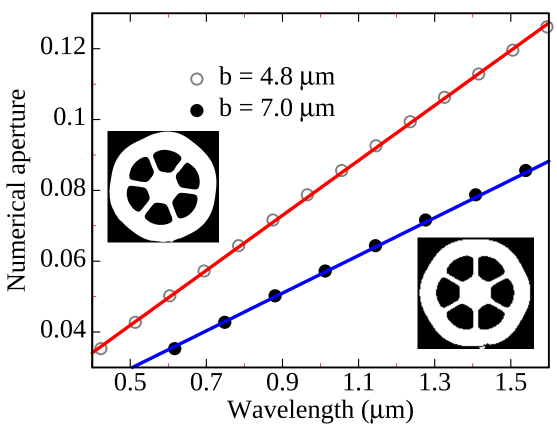

Fig. 1: Simulated NA for the 33 µm core PCF (upper left inset) with bridges of width $b \simeq 4.8$ µm and the 50 µm core PCF (lower right inset) with bridges of width $b \simeq 7.0$ µm. Note the different scale for the two insets.

3. Transmission Experiments

Assuming worst-case conditions [4], from the above NAs one can estimate a bit rate–length product of around 350 Mbit/s · km for the 50 µm fiber, whereas the 33 µm sample should have around 180 Mbit/s · km. In what follows the transmission properties of such PCFs with a length of $L = 100$ m are examined.

3.1 Small-Signal Transfer Function and DMD

In order to get a first indication of the fibers' expected transmission bandwidths, we have determined the small-signal frequency responses with a scalar network analyzer. As optical source, standard 850 nm GaAs based VCSELs have been employed. The 12 µm active diameter, oxide-confined devices show transverse multimode emission with a root mean square spectral width of less than 0.4 nm even under modulation. The lasing threshold current amounts to 1.8 mA and the bias current for the small-signal as well as data transmission experiments was chosen as 9 mA, where the 3-dB bandwidth is 8.6 GHz. At the receiving end, a multimode fiber pigtailed InGaAs pin-type photoreceiver with above 8 GHz bandwidth was used.

The left-hand side of Fig. 2 depicts the relative responses of both PCF samples. The 33 and 50 µm core diameter fibers show a bandwidth–length product of 200 and 430 MHz · km,

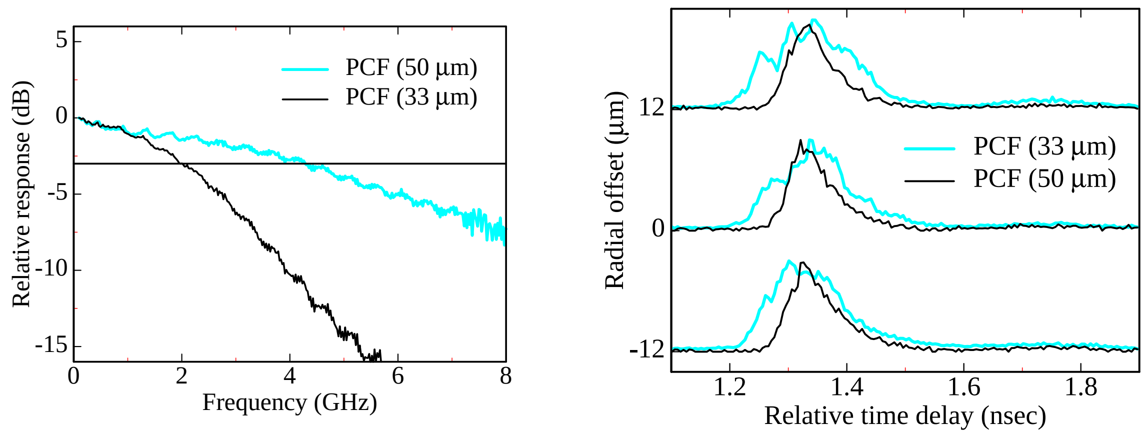

Fig. 2: Small-signal frequency responses at 850 nm for the two 100 m-long PCFs illustrated in Fig. 1 (left) and normalized DMD plots for both fibers at offset positions of −12, 0, and 12 µm (right).

respectively. These figures are significantly larger than expected from the corresponding NAs. In the next section we extend the NA estimations and show simulations of the modal time delays for the two PCFs.

In order to get quantitative insight into the modal delay properties, we have determined the PCFs differential mode delay (DMD) characteristics, see the right-hand side of Fig. 2. Here, a singlemode fiber is scanned over the PCF input and the impulse response at the output end is recorded for each offset position. A gain-switched 850 nm singlemode VCSEL delivering pulses with less than 40 ps full width at half maximum is employed for this purpose [5]. It is seen that the output pulses of the 50 µm fiber are rather narrow and virtually independent of the offset position. On the other hand, those of the 33 µm sample show larger variability and are up to twice as broad, which well supports the above observations.

3.2 Digital Data Transmission

Data transmission experiments have been carried out under non-return-to-zero $2^7 - 1$ word length pseudo-random bit sequence modulation using the aforementioned multimode VCSEL driven with 0.9 V peak-to-peak voltage. Figure 3 summarizes obtained bit error rate (BER) curves. With the smaller core diameter fiber, up to 5 Gbit/s could be transmitted without indication of a BER floor. The power penalty versus back-to-back (BTB) operation is about 3 dB at a BER of 10^{-12}. On the other hand, the 50 µm fiber even enables 10 Gbit/s transmission over $L = 100$ m length with only 2.9 dB power penalty. The observed increase in data rate is in full agreement with the small-signal and DMD measurement results.

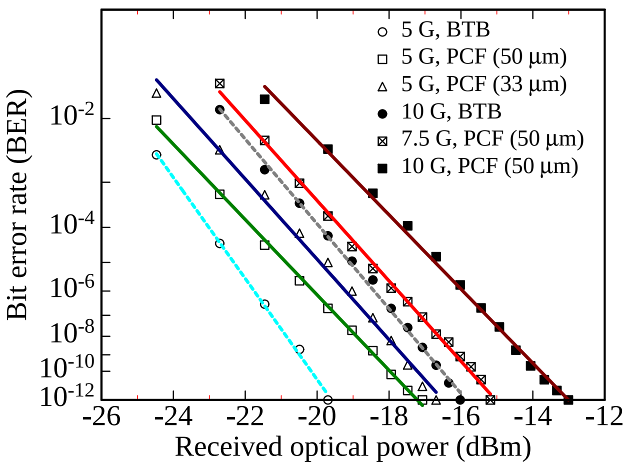

Fig. 3: BER characteristics for both 100 m-long PCFs at data rates of 5, 7.5, and 10 Gbit/s.

4. Simulations

A plane-wave method [6] is used to calculate the propagation constants $\beta_m = n_m\omega/c$ of the eigenmodes with index m, where n_m is the effective index, ω the angular frequency, and c the vacuum velocity of light. For the refractive index profile, optical micrographs are transformed to a one-bit format representing the two-component composite air–silica structure and for the refractive index a Sellmeier expression for $n(\omega)$ in silica and $n = 1$ in air is used. The simulation of Maxwell's equations for a given ω delivers sets of propagation constants $\{\beta_m\}$ and eigenfields $\{E_m\}$ where $m = 1, 2, 3, \ldots M$ with M as the number of guided eigenmodes. M is determined from the experimentally measured NA which is transformed to an effective cladding index $n_{\rm cl}$. The number of guided eigenmodes M then follows from the requirement that $c\beta_M/\omega \geq n_{\rm cl}$.

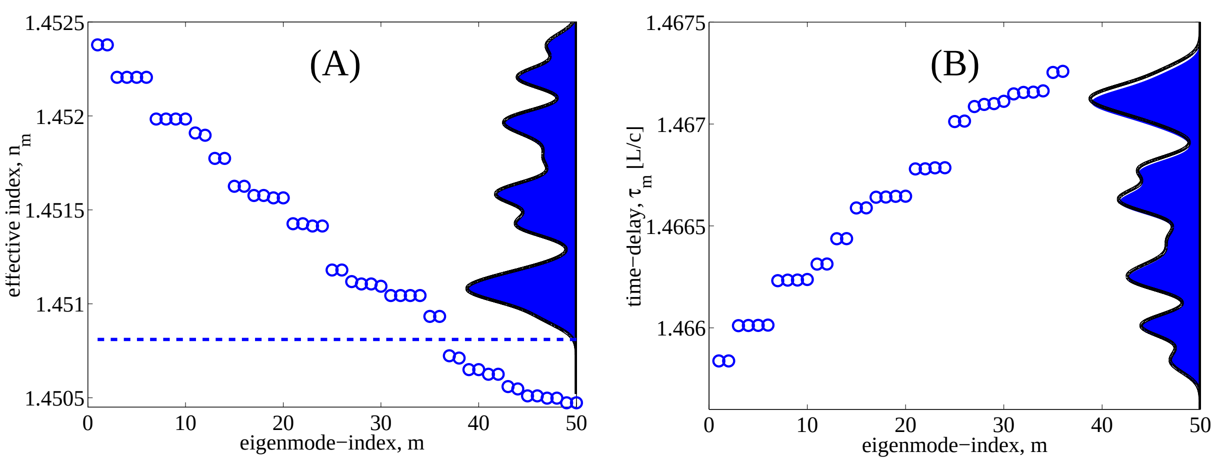

Fig. 4: Effective indices of the $M = 36$ guided eigenmodes at $\lambda = 850$ nm in a PCF with a 33 µm core (A; see upper left inset of Fig. 1). The horizontal dashed line indicates the cladding index $n_{\rm cl}$ corresponding to the experimentally measured NA. Corresponding time delays τ_m and the distribution $P(\tau_m)$ (B).

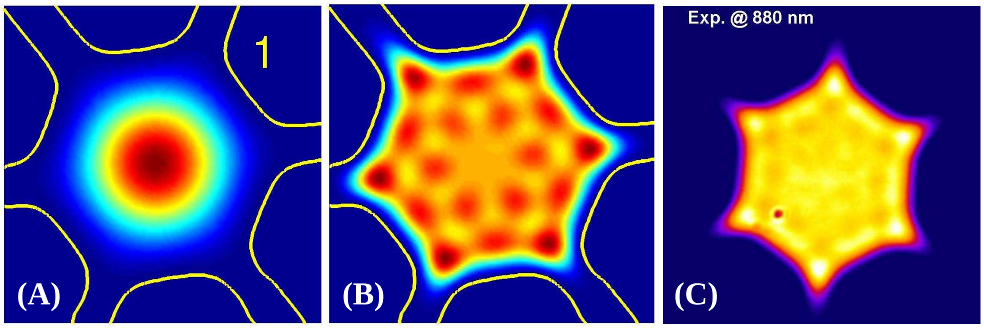

Fig. 5: Intensity distribution at $\lambda = 850\,\mathrm{nm}$ in the $33\,\mu\mathrm{m}$ PCF (see upper left inset in Fig. 1). Diagram (A) depicts the first ($m = 1$) eigenmode and diagram (B) shows the average eigenfield intensity which agrees well with the experimentally observed near-field intensity depicted in diagram (C). In diagrams (A) and (B), the contour lines indicate the air–silica interfaces.

The time delays (or group delays) are given by $\tau_m = L\partial\beta_m/\partial\omega$, where the group velocity is calculated by the approach described in Ref. [7]. The variation with m usually sets the limit on the bit rate and in that case the bit rate–length product is given by [4, 8]

$$B_T \cdot L \simeq L/\Delta T \ , \ \Delta T \approx \max\{\tau_m\} - \min\{\tau_m\}, \tag{1}$$

where ΔT is the width of the distribution $P(\tau_m)$ of the time delays. In the ray-optical picture, $\max\{\tau_m\}$ can be expressed in terms of the NA [4] and in this respect the expression is analogous to our estimations in Sect. 3 based on the NA. However, for a sufficiently low number of guided modes, quantitative differences caused by the beginning break-down of geometrical optics can be expected.

Figure 4 shows results at $\lambda = 850\,\mathrm{nm}$ for a PCF with a $33\,\mu\mathrm{m}$ core (see upper left inset in Fig. 1). Experimentally, this fiber is found to have NA $\simeq 0.07$ and the corresponding effective cladding index is indicated by the dashed line in the left diagram. For the given core size this results in $M = 36$ guided eigenmodes. Figure 4 (right) illustrates the time delays with the filled curve showing the distribution $P(\tau_m)$ (the projection of the data onto the y-axis) calculated from a superposition of Gaussians with a width given by the mean level spacing $(\tau_M - \tau_1)/(M - 1)$. We have $\Delta T \simeq 0.00087 \cdot L/c$ corresponding to $B_T \cdot L \simeq 344\,\mathrm{MHz} \cdot \mathrm{km}$ which, as expected, is somewhat larger than the NA estimate.

The total electric field E guided by the fiber is constructed by a linear combination of the eigenfields. For a not too narrow linewidth of the light source, cross-terms in $|E|^2$ might be neglected and for uniform (with respect to eigenmode index m) launch and attenuation an intensity distribution proportional to the average eigenfield intensity, i.e., $|E|^2 \approx M^{-1} \sum_m^M |E_m|^2$ is supposed to be measured. The same will be the case for arbitrary launch and strong mode mixing. As an example, Fig. 5 (A) shows the eigenfield intensity of the fundamental mode $m = 1$. The average eigenfield intensity (diagram B) compares well to the experimentally measured near-field intensity (C). This can be mainly attributed to the close-to-uniform launch of the fiber by a VCSEL since the good agreement for the bit rate suggests that the effect of mode-mixing (inter-modal diffusion) is limited.

The eigenmodes fall into different groups with different degeneracies (these degeneracies are slightly lifted due to a weakly broken symmetry in the real fiber) as evident from both the effective indices in Fig. 4 as well as the corresponding intensity plots (not shown here; see [1]). The first two eigenmodes ($m = 1, 2$) are the doubly degenerate fundamental mode corresponding to the two polarization states of the fundamental mode in standard fibers and from a practical point of view they can be considered polarization states though the "x-polarization" in principle has a very small y-component and vice versa.

5. Conclusion

For the first time, quasi error-free transmission of 10 Gbit/s digital data signals over a multimode photonic crystal fiber with 50 µm core diameter and as much as 100 m length has been demonstrated. With some optimizations concerning design and fabrication, these PCFs show good prospects as an alternative to graded-index fibers in optical datacom environments. Comparing to simulations, good agreement is found with the measured fiber bandwidths.

References

[1] N.A. Mortensen, M. Stach, J. Broeng, A. Petersson, H.R. Simonsen, and R. Michalzik, "Multi-mode photonic crystal fibers for VCSEL based data transmission," *Opt. Express*, vol. 11, pp. 1953–1959, 2003.

[2] R. Michalzik, K.J. Ebeling, M. Kicherer, F. Mederer, R. King, H. Unold, and R. Jäger, "High-performance VCSELs for optical data links," *IEICE Trans. Electron.*, vol. E84-C, pp. 629–638, 2001.

[3] P. Russell, "Review: photonic crystal fibers," *Science*, vol. 299, 2003.

[4] G.P. Agrawal, *Fiber-Optic Communication Systems*. New York: Wiley & Sons, 1997.

[5] R. Michalzik, F. Mederer, H. Roscher, M. Stach, H. Unold, D. Wiedenmann, R. King, M. Grabherr, and E. Kube, "Design and communication applications of short-wavelength VCSELs," *Proc. SPIE*, vol. 4905, pp. 310–321, 2002.

[6] S.G. Johnson and J.D. Joannopoulos, "Block-iterative frequency-domain methods for Maxwell's equations in a planewave basis," *Opt. Express*, vol. 8, pp. 173–190, 2001.

[7] J. Lægsgaard, A. Bjarklev, and S.E.B. Libori, "Chromatic dispersion in photonic crystal fibers: fast and accurate scheme for calculation," *J. Opt. Soc. Am. B*, vol. 20, 2003.

[8] A.K. Ghatak and K. Thyagarajan, *Introduction to Fiber Optics*. Cambridge: Cambridge University Press, 1998.